Supplemental Material for "Motility of acoustically powered micro-swimmers in a liquid crystalline environment"

Jaideep Katuri,[1] Andrey Sokolov,[1] and Alexey Snezhko[1]
Argonne National Laboratory, 9700 S. Cass Avenue, Lemont, IL 60439, USA

Reconstruction of the director field and the optical phase retardance

The use of a polarized camera for imaging liquid crystals allows a rapid and accurate reconstruction of the director field. The polarization sensor, consisting of a conventional light-sensitive sensor overlaid by an array of polarizers, can capture four polarized images at orientations 0^0, 45^0, 90^0, and 135^0 simultaneously. An example of a raw image is shown in S1(a). Each 2x2 pixels block (three of them are highlighted by the red square for illustration) contains information about the direction and the degree of polarization. For example, for a fully non-polarized light, all four pixels have the same brightness and for a fully polarized light, the brightness of each pixel is different with the maximum at the pixel with the polarizer oriented at the closest angle to the polarization of light. A birefringent material, such as DSCG (disodium cromoglycate) liquid crystal, alternates the polarization of light. If DSCG in the nematic phase is illuminated by the circularly polarized light and observed by the polarization camera, the local orientation of main optical axes and optical retardance, and correspondingly a director field, can be reconstructed from each 2x2 pixels block by using simple linear algebra and treating liquid crystal as a linear phase retarder. An example of such reconstruction is shown in Fig S1(c).

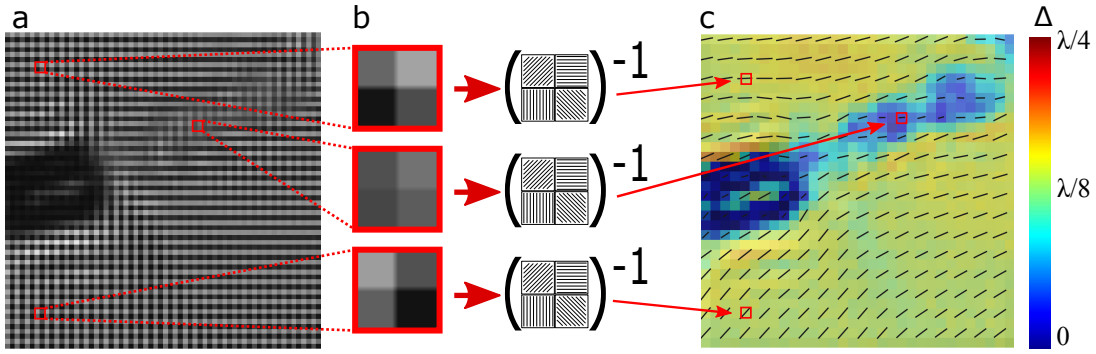

FIG. S1. Illustration of the nematic field reconstruction process. (a) An image captured by the polarized camera. (b) Intensities of the observed signal at each pixel of calculation units (three 2x2 pixels blocks are selected for illustration purpose located at different places in the original image (a)) are used to calculate the local director field and the optical retardance. (c) The final image. The director field is depicted by short black lines and the color illustrates the phase retardance.

Intuitive stabilization mechanism for a perpendicular swimmer

According to our experimental observations, a significant fraction of swimmers tends to move perpendicular to the director field in LC, in contrast with bacterial swimmers. Such behavior may seem very puzzling since perpendicular swimming creates a much larger elastic deformation of nematic order. Indeed, if no energy is ejected into the system, the rod shape particle will align with the director field to minimize the free energy. However, the high-frequency oscillation of the air-bubble interface in LC may induce flows that create a rotating torque T on the swimmer and orient it perpendicular to the director field. This mechanism is schematically presented in Fig. S2 (a,b). The flow created by the swimmer oriented at a certain angle relative to the director field is redirected and split into two jets due to anisotropy in viscosity. At the approximation that the viscosity and elasticity perpendicular to the director field is much larger than the parallel, we can suggest a simple analogy of a water jet hitting a hard wall at a certain angle. Using this analogy we may assume that the flow V_2 is larger than V_1 since its direction is better aligned with the direction of the original flow. The resulting propulsion force is not aligned with the swimmer body and creates a rotating torque T. This torque is canceled when the swimmer becomes oriented perpendicular to the director field.

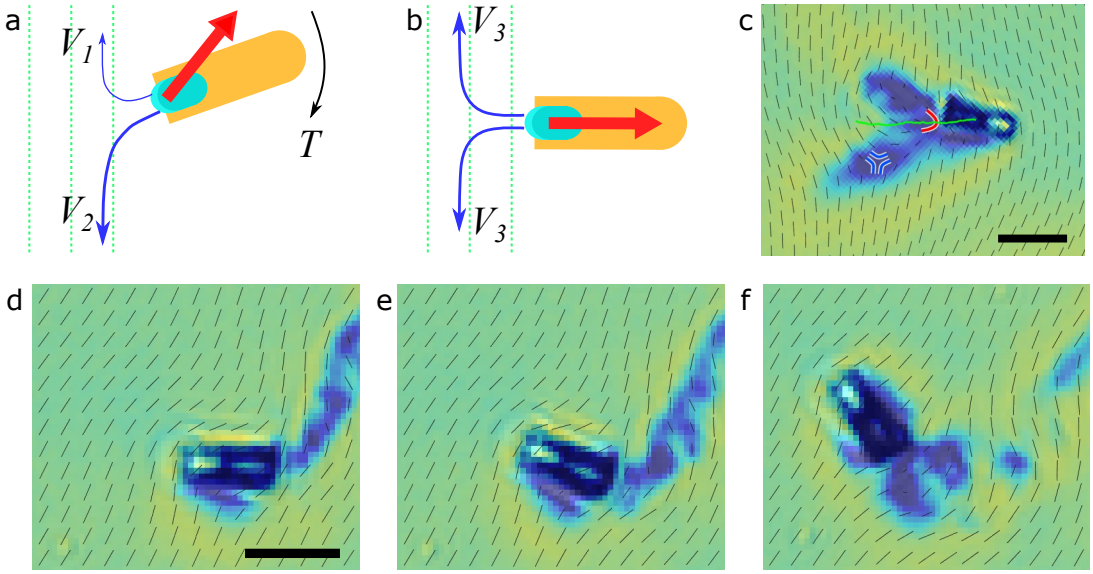

FIG. S2. Stabilization mechanism for perpendicular swimmers. (a-b) Simplified schematic of flow structure created by s swimmer moving at different angles relative to the director field. The director field is shown by green dashed lines. The blue lines with arrows depict flows created by the oscillating air-LC interface. The self-propelling force is shown in red. (c) An experimental picture of a swimmer self-propelling perpendicular to the director field. Short black lines depict the director field. The blue background color indicates areas with the reduced order parameter (melted LC). The trajectory of the swimmer is marked by the green line. (d-e) Snapshots of the director field in the vicinity of a swimmer during the transition from parallel to perpendicular swimming. The scale bar is 15 μm.

To obtain the experimental evidence of flow separation we analyzed the order parameter in the vicinity of the swimmer moving perpendicular to the director field, see Fig. S2(c) and Movies 2 and 7. The optical retardance and, correspondingly, the order parameter are reduced at the tail of the swimmer in the shape of "V". In our experiments, such a structure of melted LC is very typical for a perpendicular swimmer. Assuming that the liquid crystal is melted by high amplitude microscopic flows, our observation confirms that the perpendicularly oriented director field indeed splits and redirects the flow created by the air-bubble interface.

Interactions of acoustic bubble swimmers with topological defects

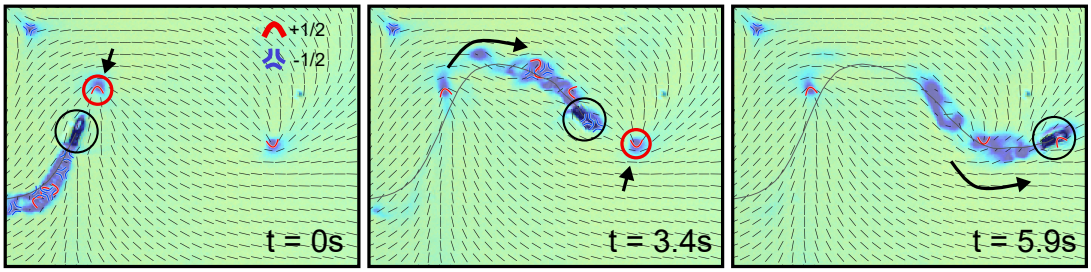

FIG. S3. Interaction of an acoustic swimmer with topological defects. The snapshots show the time progression as the trajectory of the acoustic swimmer is deflected upon interactions with two +1/2 defects. The black circle marks the location of the swimmer. The red circles and the arrows point to the +1/2 defects that the acoustic swimmers interact with.

Previous experiments with motile bacteria have shown that the bacteria get trapped and accumulate in the core of +1/2 topological defects and are depleted from the cores of -1/2 defects as they are redirected by the nematic field around the defect[1]. We find that the acoustic swimmers also respond to the presence of topological defects in nematic media. However, unlike bacteria whose propulsive force is insufficient to escape from the +1/2 defect, the acoustic swimmers are not trapped by the +1/2 defects. For both the case of +1/2 and -1/2 defects, we observe scattering events where the trajectory of the swimmer is deflected in the presence of a defect, Fig. S3 (Also, see Movie 5 and 6).

We also observe that, while swimming at a distance (1-2 body lengths) from the defects, acoustic swimmers can draw nearby topological defects towards them through hydrodynamic flows and carry them along the swimmer trajectory, see Movie 7.

Director field around a swimmer before and immediately after the application of the acoustic field

A colloidal particle immersed in the liquid crystal frequently triggers the formation of defects near its surface such as Saturn rings or monopoles[2–6]. Our experimental observations and the used technique for reconstruction of the director field do not reveal the existence of topological defects in the vicinity of an inactive swimmer while the acoustic field is not applied (Fig. S4a). However, the topological defects may arise upon the application of the acoustic field due combination of two effects - locomotion of the swimmer and microstreaming. The microscopic flows and jets produced by the oscillating air bubble chaotically disturb the director field behind the swimmer (Fig. S4b) creating topological defects (Fig. S4c)and then advecting them (Fig. S4d) into the direction opposite to the swimming direction.

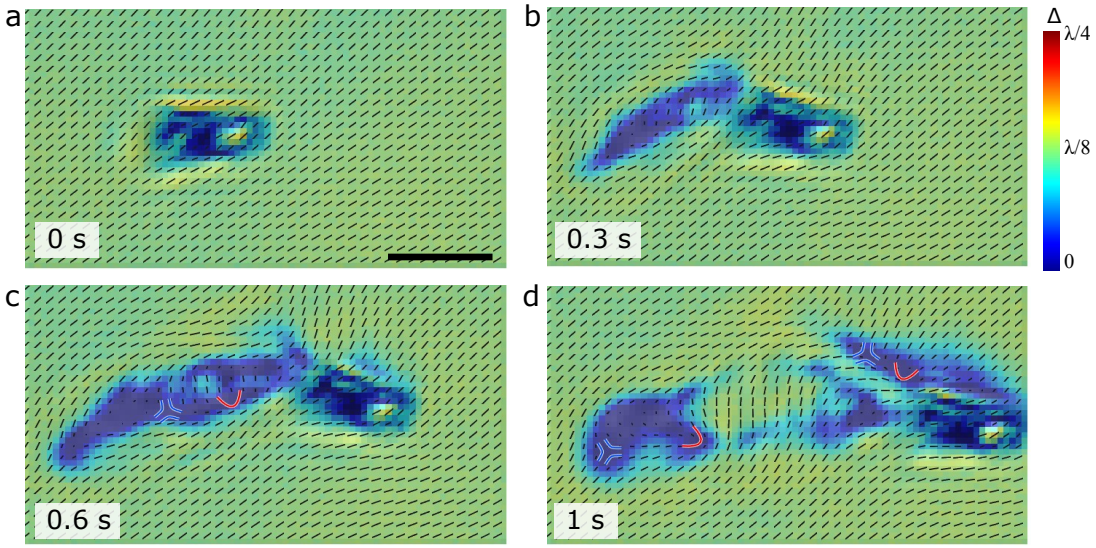

FIG. S4. The director field, the order parameter distribution and topological defects in the vicinity of a swimmer upon application of the acoustic field. Frames (a-d) illustrates the states before acoustic field is applied, and 0.3 s, 0.6 s, and 1 s after the acoustic field is turned on. The color illustrates the optical phase retardance and short black line depicts the director field.

Movies description

For all movies short black lines depict the director field and the color illustrates the local optical retardance. Blue color areas correspond to areas with reduced retardance and, correspondingly, reduced order parameter (melted LC). All movies are recorded at 10 frames per second.

Movie 1. Example of a chaotic behavior of a bubble swimmer. V = 15V_{pp}; f = 900-1400 kHz sweep (50 ms) The playback speed is 25 frames/s.

Movie 2. The transition from parallel swimming to perpendicular and back. V = 10V_{pp}; f = 900-1120 kHz sweep (50 ms) The playback speed is 25 frames/s.

Movie 3. Unstable swimming under a single frequency acoustic wave. The swimmer slows down and becomes non-motile. When the frequency is shifted slightly (at 0:14), the swimming resumes. V = 12V_{pp}; f = 1120 kHz. The playback speed is 25 frames/s.

Movie 4. Backward swimmer. The swimmer is moving towards the side with the bubble. Several defects are transferred by the swimmer. V = 15V_{pp}; f = 900-1400 kHz sweep (50 ms). The playback speed is 25 frames/s.

Movie 5. Scattering of a swimmer on two positive defects. V = 15V_{pp}; f = 900-1200 kHz sweep (50ms). The playback speed is 10 frames/s.

Movie 6. Scattering of a swimmer on a negative defect. Transition from a parallel to a perpendicular motion. The playback speed is 10 frames/s. V = 15V_{pp}; f = 900-1200 kHz sweep (50ms).

Movie 7. Transition from parallel to perpendicular swimming is accompanied by the separation of microstreaming flow into several jets redirected by director field and emerged topological defects. The playback speed is 10 frames/s. V = 15V_{pp}; f = 900-1200 kHz sweep (50ms).

[1]M. M. Genkin, A. Sokolov, O. D. Lavrentovich and I. S. Aranson, *Physical Review X*, 2017, **7**, 011029.
[2]E. Terentjev, *Physical Review E*, 1995, **51**, 1330.
[3]R. Ruhwandl and E. Terentjev, *Physical Review E*, 1997, **56**, 5561.
[4]O. Mondain-Monval, J. Dedieu, T. Gulik-Krzywicki and P. Poulin, *The European Physical Journal B-Condensed Matter and Complex Systems*, 1999, **12**, 167–170.
[5]I. Muševič, *Materials*, 2017, **11**, 24.
[6]J. Loudet, *Liquid Crystals Today*, 2005, **14**, 1–14.